Productive infection of primary human hepatocytes with SARS-CoV-2 induces antiviral and proinflammatory responses

We read with interest the article by Luxenburger and Thimme, summarising current knowledge about hepatic sequelae in the context of SARS-CoV-2 infection.[1] As acute liver injury is observed in one-third of the patients with hospitalised COVID-19[2 3] and chronic liver disease is associated with higher mortality rates,[4] a detailed understanding of hepatic susceptibility and dysfunction in the context of SARS-CoV-2 infection is of utmost importance. Previous studies have provided evidence of hepatic infection,[5–7] however, the molecular mechanisms underlying acute liver injury associated with SARS-CoV-2 infection are not well understood. Here we show that primary human hepatocytes (PHH) can be productively infected with SARS-CoV-2. Donor-specific production kinetics were observed, with de novo viral secretion from PHH increasing in a time-dependent manner for four out of six donors (figure 1A). To explore virus replication and host gene dysregulation in parallel, Illumina sequencing of time point-matched infected and uninfected PHH was performed, followed by mapping to host and virus scaffolds. Increases in viral genome coverage over time corresponded to increasing rates of secreted virus (figure 1B). On the host side, detectable messenger RNA (mRNA) expression of known or suspected SARS-CoV-2 entry factors was observed for all PHH donors (figure 1C). Despite robust viral replication, host transcriptional responses were delayed until 72 hours post infection (hpi) and correlated with specific type III and interferon-β (IFN) induction in three donors (D1–3; termed reactive), while two donors remained unreactive, even though low levels of viral replication were observed (D4–5; figure 1C). These observations imply a viral replication threshold must be crossed to trigger robust host responses in PHH. Interestingly, one donor (D6; termed pre-activated) possessed abundant IFN-encoding transcripts independent of infection status or sampling time, resulting in high baseline interferon stimulated gene expression which prevented productive infection (figure 1A–C). Of note, similar to reactive donors at 72 hpi, IFN production in the pre-activated donor was also limited to IFN-β and IFNL1-4, suggesting hepatocytes are unable to produce additional IFN types/subtypes at meaningful levels.

To further dissect host responses to productive infection, we focused on the three reactive donors (D1–3) and observed significant host responses 72 hpi (figure 2A,B), compared with the two unreactive donors (online supplemental figure 1A-D). Further analyses confirmed a broad infection-induced reprogramming of the hepatocyte transcriptional landscape at 72 hpi in the reactive donors (figure 2). This included significant upregulation of nucleic acid sensors and transcription factors, antiviral effectors and factors associated with inflammatory responses and cell chemotaxis (figure 2C,D). We also observed an increased expression of markers associated with necrotic and programmed cell death, as well as regulation of blood coagulation, implying direct hepatic damage due to viral replication (figure 2D). To further investigate hepatic sequalae following SARS-CoV-2 infection, we compared our data set with host responses in PHH following hepatitis C virus (HCV) infection,[8] which causes a chronic infection of the liver in >80% of cases. Interestingly, shared and virus-specific host signatures were observed (figure 2E,F). As previously described, HCV infection uniquely targeted gene programmes associated with translational shutoff, which may contribute to liver persistence and amelioration of cytolytic responses and were not observed in SARS-CoV-2 infection (figure 2F). The shared terms dysregulated by both viruses exhibited substantial overlap and were associated with IFN signalling, canonical antiviral and proinflammatory responses and cell-death, highlighting similarities in early host responses to divergent viruses that cause chronic and acute infections. Interestingly, SARS-CoV-2 infection of PHH uniquely dysregulated gene classes associated with blood coagulation, chromatin remodelling and circadian rhythm, which was not observed during HCV infection and requires further investigation (figure 2F). In conclusion, our data demonstrate donor-specific susceptibilities towards hepatic SARS-CoV-2 infection. SARS-CoV-2 viral replication and its associated cytotoxicity within the liver may result in virus-mediated damage, immune-mediated inflammatory responses and could further contribute to hepatic impairment, accounting for clinical observations. However, robust host responses to infection in the liver may also be protective, ultimately promoting clearance and priming downstream adaptive immunity. Our data therefore emphasise potential multimodal effects following hepatic SARS-CoV-2 infection and highlight primary human hepatocytes as suitable model for ex vivo exploration of hepatic sequelae following COVID-19 infection.

MATERIALS AND METHODS

Primary human hepatocytes

PHH were purchased from PRIMACYT Cell Culture Technology GmbH as cryopreserved hepatocytes and thawed according to the manufacturer's instructions. All patients (table 1, online supplemental table S1) were serologically tested negative for HIV, hepatitis B, hepatitis C and SARS-CoV-2. PHHs were seeded at a density of $1.6–2.4\times10^5$ cells/cm^2 on collagen-coated 12-well plates 1-day prior to infection and were kept in Human Hepatocyte Maintenance Medium (PRIMACYT) in a 5% CO_2 incubator at 37 °C.

Ethical compliance

The used PHH are commercially available and distributed by PRIMACYT Cell Culture Technology GmbH. Patients informed consent was obtained by PRIMACYT, as stated on their website. The tissue is removed during surgery and would otherwise be discarded as biological waste. All provided information within this manuscript is publicly available on their website.

SARS-CoV-2 infection

SARS-CoV-2 wildtype (WT) virus isolate (B1.1.70, GISAID accession ID: EPI_ISL_1118929) was obtained as previously described.[9] Cells were infected with 42 500 plaque forming units (PFU)/cm^2 at 37 °C for 2 hours. After washing thrice with phosphate-buffered saline, the cells were incubated at 37 °C in a humidified atmosphere for 24 hours, 48 hours or 72 hours. At the indicated time points, supernatants were harvested and titrated via a limiting dilution assay. Cell lysates were harvested in the RA1 lysis buffer (Macherey Nagel) prior to RNA extraction. To increase RNA yields, RNA was isolated after one freeze-thaw cycle, additional shredding with a narrow bore syringe and clearing of the lysate with a NucleoSpin Filter column (Macherey Nagel). Afterwards, RNA was isolated with the NucleoSpin RNA kit (Macherey Nagel) according to the manufacturer's instruction.

Library preparation and RNA sequencing

Common libraries were prepared using an Illumina Stranded mRNA Prep kit using 200 ng of RNA according to the manufacturer's instructions. Libraries were

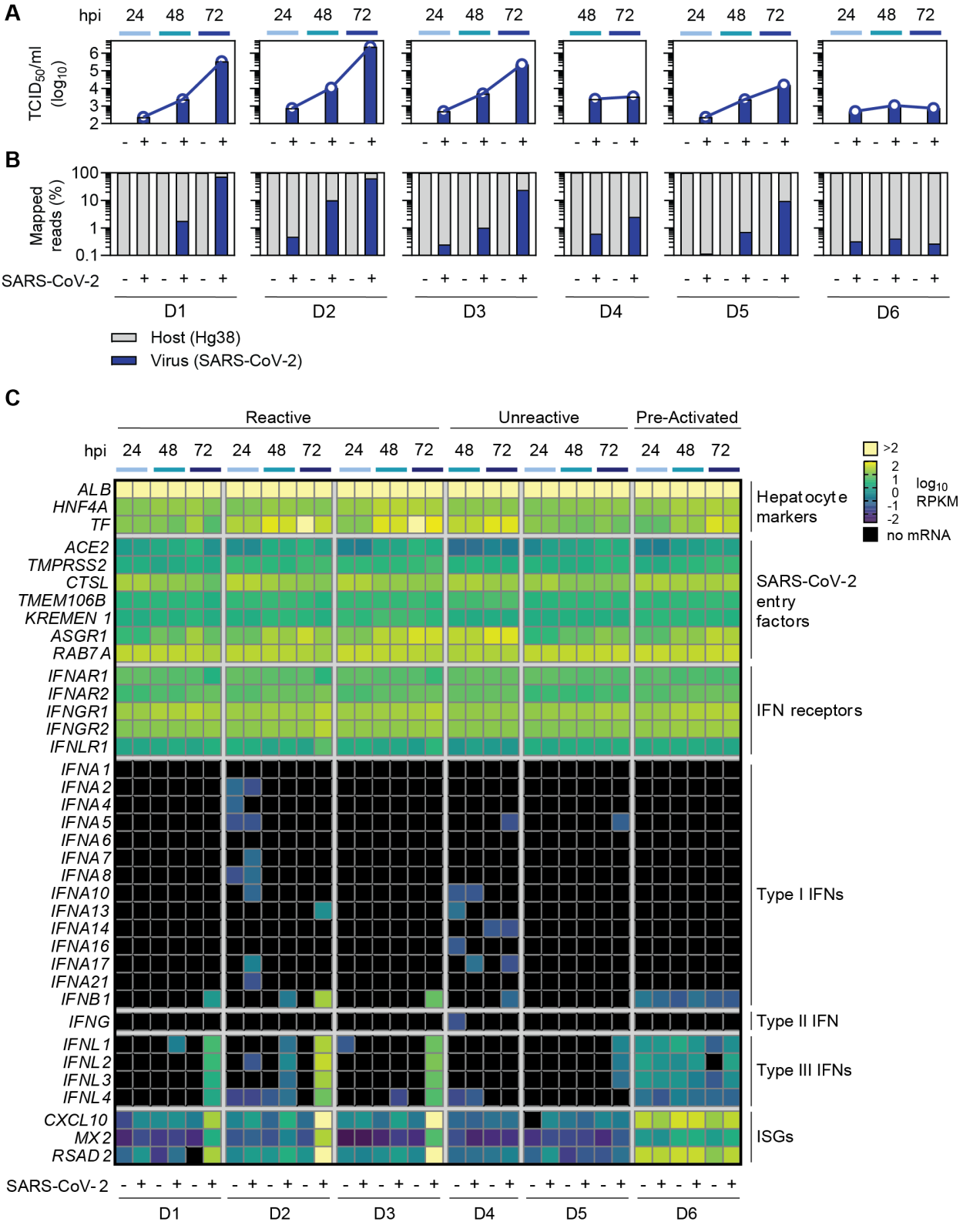

Figure 1 Productive SARS-CoV-2 infection of PHH strongly induces selected interferons (IFNs). (A) Secretion of infectious virions from SARS-CoV-2-infected PHH at the indicated time points (n=6 donors). (B) Host-mapped and virus-mapped reads (% of total) derived from SARS-CoV-2-infected PHH at the indicated time points (n=6 donors). (C) Heat maps of indicated control gene expression (log_{10} RPKM values) from individual PHH donors. Robust *IFNB1* and *IFNL1-4* induction is clearly observed in three donors at 72 hpi (D1–3, reactive). No IFN induction is observed in two donors at 72 hpi (D4–5, unreactive). One donor (D6) displayed pre-activated *IFNB1* and *IFNL1-4* and high intrinsic ISG levels, independent of infection status. hpi, hours post infection; ISG, interferon stimulated gene; mRNA, messenger RNA; PHH, primary human hepatocytes; RPKM, reads per kilobase per million mapped reads; TCID50, 50% tissue culture infectious dose.

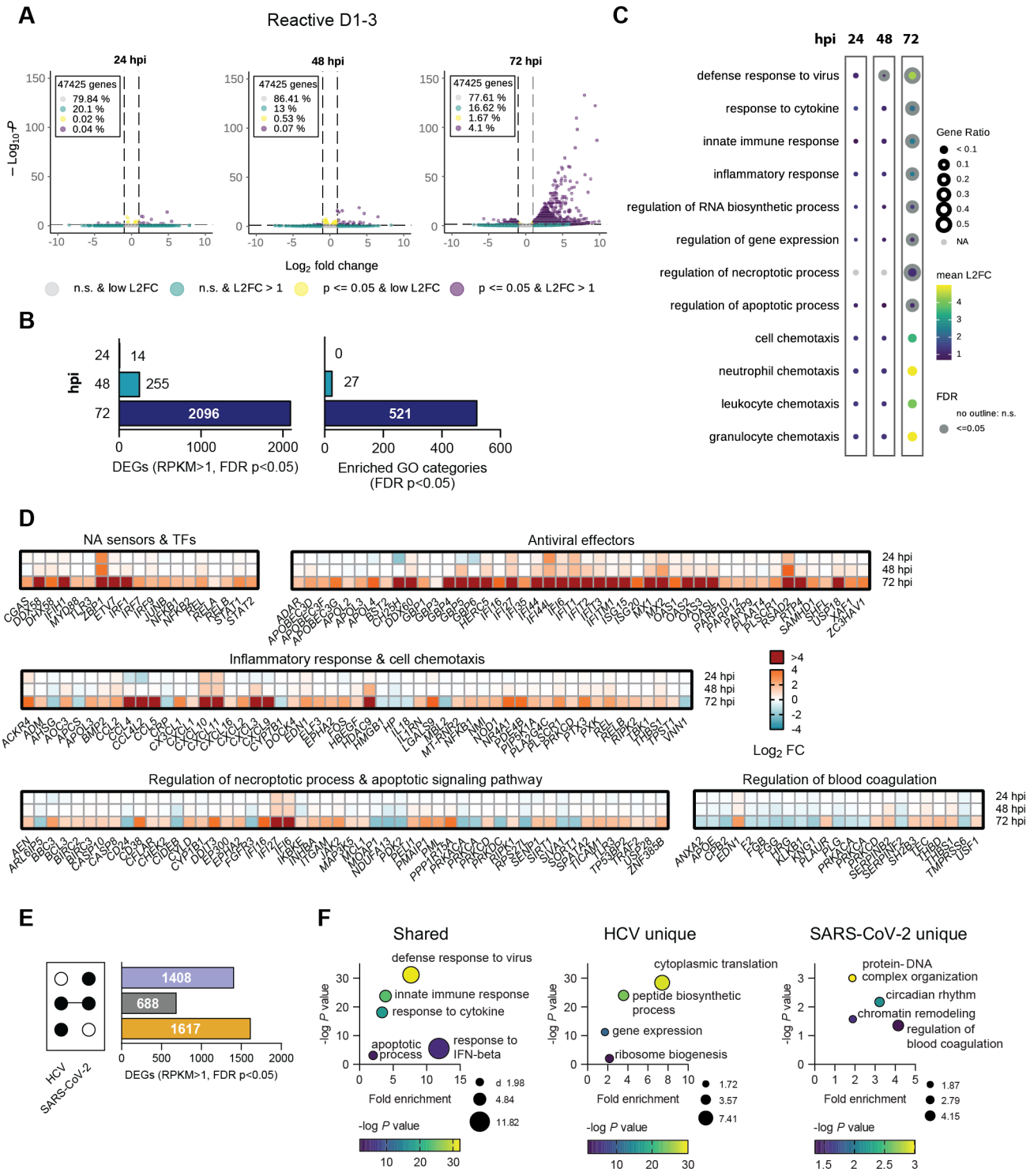

Figure 2 SARS-CoV-2 induces a functionally diverse transcriptional programme in PHHs. (A) Volcano plots highlight numbers of significantly dysregulated transcripts from the three reactive PHH donors (D1–3) at the indicated time points. (B) Numbers of SARS-CoV-2-induced differentially expressed genes (DEGs; left) and enriched Gene Ontology (GO terms; right) at the indicated time points (n=3 reactive donors; D1–3). (C) Enriched GO terms in SARS-CoV-2-infected PHHs at 72 hpi encompass diverse biological processes (12 representative categories shown). (D) Heat maps depict SARS-CoV-2 induced transcripts at 24, 48 and 72 hpi associated with the indicated categories (means from n=3 reactive donors; D1–3). For each heat map, all transcripts presented are significantly dysregulated at 72 hpi (FDR p<0.05). (E) Upset plot highlights overlapping and distinct DEGs induced by SARS-CoV-2 and HCV at 72 hpi (RPKM>1 FDR p<0.05). (F) Representative GO terms, enriched after either SARS-CoV-2 or HCV infection of PHH, or shared between both viruses. FC, fold change; FDR, false discovery rate; HCV, hepatitis C virus; hpi, hours post infection; NA, nucleic acid; PHH, primary human hepatocytes; RPKM, reads per kilobase per million mapped reads; TF, transcription factor.

Table 1 PHH donors purchased from PRIMACYT Cell Culture Technology GmbH

PHH donor	Company lot #	Cause of death/ pathology
D1	CyHuf19002	Hepatic metastases
D2	CHM2225-He-Z	Hepatocellular carcinoma
D3	NHM2251-HE-N	Head trauma
D4	CHM2221-HE-C	Cholangiocarcinoma
D5	CyHum19008-HE-C	Liver mass
D6	NHM2252-HE-N	Anoxia

PHH, primary human hepatocytes.

sequenced as paired ended by Illumina NextSeq 1000 Sequencing Systems under Illumina DRAGEN BCL Convert - 3.8.4 Application.

Data analyses

Mapping of fastq files generated for 36 individual samples was performed against the human (hg38) and SARS-CoV-2 (B.1 D614G) reference genomes using CLC Genomics Workbench 23.0.5 (Qiagen). Relative transcript expression was calculated from raw count data via normalisation to gene length and total reads per sample (reads per kilobase per million mapped reads) to allow for comparison between samples. Identification of DEGs and enriched GO categories at individual time points for donors D1–3 were calculated in CLC Genomics Workbench or using the Gene Ontology Resource (https://geneontology.org/). Volcano plots were generated using the R package 'EnhancedVolcano' V.1.16.0. Volcano and GO enrichment plots were generated or improved using the R package 'ggplot2' V.3.4.1 or using GraphPad Prism V.10.0.3.

Natalie Heinen ,[1] **Rajendra Khanal**,[2,3] **Saskia Westhoven**,[1] **Mara Klöhn**,[1] **Simon T Herrmann**,[1] **Maike Herrmann**,[4] **Tran Tuoc**,[5] **Pauline Antonie Ulmke**,[5] **Hoang Duy Nguyen**,[5] **Huu Phuc Nguyen** ,[5] **Eike Steinmann** ,[1,6] **Daniel Todt** ,[1,7] **Richard J P Brown** ,[1,4] **Amar Deep Sharma** ,[2,3] **Stephanie Pfaender** [1]

[1]Department for Molecular and Medical Virology, Ruhr University Bochum, Bochum, Germany
[2]Department of Gastroenterology, Hepatology, Infectious Diseases and Endocrinology, Hannover Medical School, Hannover, Germany
[3]Research Group RNA Therapeutics & Liver Regeneration, REBIRTH-Research Center for Translational Regenerative Medicine, Hannover Medical School, Hannover, Germany, Hannover Medical School, Hannover, Germany
[4]Division of Veterinary Medicine, Paul-Ehrlich-Institute, Langen, Germany
[5]Department of Human Genetics, Ruhr University Bochum, Bochum, Germany
[6]German Centre for Infection Research (DZIF), External Partner Site, Bochum, Germany, Bochum, Germany
[7]European Virus Bioinformatics Center (EVBC), Jena, Germany

Correspondence to Professor Stephanie Pfaender and Dr Richard J P Brown, Department for Molecular and Medical Virology, Ruhr University Bochum, Bochum, Germany; stephanie.pfaender@rub.de, richard.brown@ruhr-uni-bochum.de and Professor Amar Deep Sharma, Department of Gastroenterology, Hepatology, Infectious Diseases and Endocrinology, Hannover Medical School, Hannover, Germany; sharma.amar@mh-hannover.de

X Stephanie Pfaender @StephaniePfaen1

Acknowledgements We thank all members of the Department for Molecular and Medical Virology at the Ruhr University Bochum for their helpful suggestions and discussions.

Contributors RJPB, ADS and SP conceived the idea, designed the study and provided the conceptual framework for the study. NH, RK, SW, MK, SH, TT, PAU and HDN performed the experiments and analysed the data with help of MH, DT and RJPB. ES and HPN provided resources. SP, NH and RJPB wrote the manuscript. ES, DT and HPN provided a conceptual evaluation of the project. All authors commented on and approved the final version of the manuscript.

Funding DT was supported by a Grant from the German Federal Ministry of Education and Research (BMBF, project: VirBio, Grant number: 01KI2106). RJPB was supported by Zoonoses Platform/BMBF grant VIRASCREEN (01KI2113). RK was supported by a fellowship of the DAAD and was a member of Hannover Medical School's international PhD Program 'Infection Biology'. ES was supported by the VIRus ALlianz (VIRAL) of North Rhine-Westphalia, Ministry of Labor, Health and Social Affairs of the State of North Rhine-Westphalia (grant number CP2-1-1B) and by a grant from the German Research Council (DFG, grant number STE 1954/8-1). ADS is supported by funding from the German Research Council (DFG SH640/6-1 and Heisenberg grant DFG SH640/8-1). SP was funded by the Deutsche Forschungsgemeinschaft (DFG, German Research Foundation – 462165342).

Competing interests None declared.

Patient consent for publication Not applicable.

Ethics approval Not applicable.

Provenance and peer review Not commissioned; internally peer reviewed.

The authors declare that data supporting the findings of this study are available within the article and its supplementary information files. RNA-Seq data presented in this study are deposited in the SRA database under the accession number PRJNA1045232.

► Additional supplemental material is published online only. To view, please visit the journal online (http://dx.doi.org/10.1136/gutjnl-2023-330961).

NH and RK are joint first authors.

RJPB, ADS and SP are joint senior authors.

To cite Heinen N, Khanal R, Westhoven S, *et al*. *Gut* 2024;**73**:e14.

Received 21 August 2023
Accepted 3 December 2023
Published Online First 12 December 2023

Gut 2024;**73**:e14. doi:10.1136/gutjnl-2023-330961

ORCID iDs
Natalie Heinen http://orcid.org/0000-0003-0906-5073
Huu Phuc Nguyen http://orcid.org/0000-0001-6139-788X
Eike Steinmann http://orcid.org/0000-0002-3654-9965
Daniel Todt http://orcid.org/0000-0002-3564-1014
Richard J P Brown http://orcid.org/0000-0002-3292-6671
Amar Deep Sharma http://orcid.org/0000-0003-3599-2372
Stephanie Pfaender http://orcid.org/0000-0002-3957-5448

REFERENCES

1 Luxenburger H, Thimme R. SARS-Cov-2 and the liver: clinical and immunological features in chronic liver disease. *Gut* 2023;72:1783–94.
2 Jothimani D, Venugopal R, Abedin MF, *et al*. COVID-19 and the liver. *J Hepatol* 2020;73:1231–40.
3 Zhang C, Shi L, Wang F-S. Liver injury in COVID-19: management and challenges. *Lancet Gastroenterol Hepatol* 2020;5:428–30.
4 Marjot T, Webb GJ, Barritt AS, *et al*. COVID-19 and liver disease: mechanistic and clinical perspectives. *Nat Rev Gastroenterol Hepatol* 2021;18:348–64.
5 Fiel MI, El Jamal SM, Paniz-Mondolfi A, *et al*. Findings of hepatic severe acute respiratory syndrome Coronavirus-2 infection. *Cell Mol Gastroenterol Hepatol* 2021;11:763–70.
6 Wang Y, Liu S, Liu H, *et al*. SARS-Cov-2 infection of the liver directly contributes to hepatic impairment in patients with COVID-19. *J Hepatol* 2020;73:807–16.
7 Wanner N, Andrieux G, Badia-I-Mompel P, *et al*. Molecular consequences of SARS-Cov-2 liver Tropism. *Nat Metab* 2022;4:310–9.
8 Tegtmeyer B, Vieyres G, Todt D, *et al*. Initial HCV infection of adult hepatocytes triggers a temporally structured transcriptional program containing diverse Pro- and anti-viral elements. *J Virol* 2021;95:e00245-21.
9 Meister TL, Fortmann J, Todt D, *et al*. Comparable environmental stability and disinfection profiles of the currently circulating SARS-Cov-2 variants of concern B.1.1.7 and B.1.351. *J Infect Dis* 2021;224:420–4.